

AUTOMATIC EXTRACTION OF TREES FROM AERIAL IMAGES AND SURFACE MODELS

Bernd-M. Straub

IPI, Institute of Photogrammetry and GeoInformation, University of Hannover,
Nienburger Straße 1, 30167 Hanover, Germany, benz@ipi.uni-hannover.de

Commission III, WG 4

KEY WORDS:

Forestry, Urban, Extraction, Algorithms, Scale Space, Automatic, Tree, Snakes

ABSTRACT:

In this paper we present an approach for the automatic extraction of trees and the boundaries of the tree's crowns. The approach is based on a multi-scale representation of an orthoimage and a surface model in Linear Scale Space. The idea of the approach is that the coarse structure of the crown can be approximated with the help of a sphere or an ellipsoid. This assumption is true, if the fine structure of the crown is ignored and the coarse structure is revealed in an appropriate level of the multi-scale representation of the surface model. But this scale level is unknown, because it is correlated with the unknown diameter of the crown. The proposed solution of this chicken-and-egg problem is to investigate a wide range of scale levels, and to select the best hypothesis for a crown from all these scale levels. The segmentation of the surface model is performed using the watershed transformation. The boundary of every crown is measured with Active Contours (Snakes). The approach was tested with surface models of different resolutions (0.25 m and 1 m) and different sensors, laser scanner and image matching. An overview of the approach is given in the paper and important points are discussed.

1. INTRODUCTION

In this paper we present a new approach for the automatic extraction of individual trees using a true orthoimage and a surface model as input data. The approach is based on a segmentation in multiple scales followed by an optimisation step using Active Contours. The mathematical reasoning is mainly based on differential geometry. The surface model is used as main source of information for the extraction of the individual trees, additional colour information from the orthoimage is used to differentiate between vegetation and other objects in the scene. The aim of the approach is to detect every tree in the observed part of the real world and to measure the boundary of its crown. If the positions and the boundaries of the visible trees are known, then the crown diameter and additional descriptors concerning the shape of the crown can be derived. The height above the ground can be estimated if the ground is visible close to the crown's boundary. These parameters can be used to estimate the stem diameter in breast height, the individual surface of the crown, and the stem volume. Because most of these parameters are not visible in aerial imagery, they are usually estimated by means of statistical models (Hyypä et al. 2000).



Figure 1: 3D view of virtual trees

Based on the position and the boundary of the measured trees one can build simple virtual trees for visualisation purposes, for example as additional information in 3D city models. The

3D view in Figure 1 was generated using a scalable template¹. The virtual trees were placed onto the orthoimage with the help of the position of the automatically extracted trees. The height of the virtual trees is assumed to be proportional to the measured diameter. The 3D model is an optional output of the algorithm which is described in this paper.

In the next section of the paper a short overview is given on the related work in the field of the automatic extraction of trees in forests and settlement areas. In the main section of the paper describes the approach, it is divided in two sub sections: The first one depicts the object model for trees and the second one the processing strategy. In the last section we show some exemplary results. We close with a short summary and an outlook.

2. RELATED WORK

Trees are important topographic objects in different fields of applications. Not only ecological aspects constitute the interest in trees but also different economic factors. Obviously, data about trees play an important role in forest inventories and forestry GIS applications. In forest inventories trees are counted and parameters like height and stem diameter are measured. The first trial to utilize an aerial image for forest purposes was performed in 1897 (Hildebrandt 1987). Since that time the scientific forest community is working on methods for the extraction of tree parameters from aerial images. The early work was on the manual interpretation of images for forest inventory (Schneider 1974), (Lillesand & Kiefer 1994). The pioneers in the field of the automation of the interpretation task "extraction of individual trees from images" proposed first approaches about one and a half decade ago (Gougeon & Moore 1988), (Pinz 1989). Recent work in the field was published in (Pollock 1996), (Brandtberg & Walter 1998), (Larsen 1999), (Andersen et al. 2002), (Persson et al. 2002).

¹ The tree template is described in (Saint John 1997).

Some of the recent publications are described in detail in the following section.

A common element of the most approaches is the geometric model of a tree as it was proposed by R.J. Pollock in (Pollock 1994) (Pollock 1996). In the following, this surface description is assigned as *Pollock-Model*, and the corresponding synthetic trees as *Pollock-Trees*.

$$h: \mathbb{Z}^2 \rightarrow \mathbb{Z}^3, h(\vec{x}) = \left[a^n \left(1 - \frac{(x^2 + y^2)^{\frac{n}{2}}}{b^n} \right) \right]^{\frac{1}{n}}, \vec{x} = \begin{bmatrix} x \\ y \end{bmatrix} \quad (1)$$

The parameter a corresponds to the height, and b to the radius of the crown, n is a shape parameter. Two different surfaces which can be described with Equation 1 are depicted in Figure 2: The left one is an example for a deciduous tree, and the right one for a coniferous.

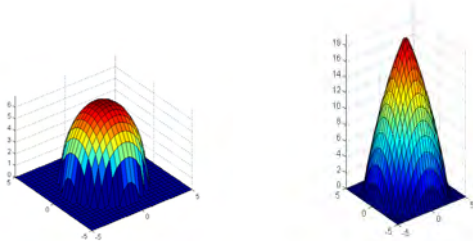


Figure 2: 3D visualisation of the Pollock-Model. Left: Surface model of a typical deciduous tree: $a=7$, $b=3.5$, $n=2.0$ Right: Coniferous tree: $a=20.0$; $b=5.0$; $n=1.2$.

The surface of a real tree is of course very noisy in comparison to the Pollock-Model. This noise is not caused by the measurement of the surface. It is simply a consequence of using such a model for a complex shape like the real crown of a tree. But the main shape of the crown is well modelled with this surface description.

In general, there are two possibilities to build a strategy for the automatic extraction of trees from the image data. The first possibility is to model the crown in detail: one could try to detect and group the fine structures in order to reconstruct the individual crowns. The second possibility is to remove the fine structures from the data with the aim to create a surface which has the character of the Pollock-Model. In the literature exist examples for both strategies: In (Brandtberg 1999) it was proposed to use the typical fine structure of deciduous trees in optical images for the detection of individual trees. It seems that this strategy works only for deciduous trees, the fine structure of a coniferous tree is not really pronounced. The other strategy, the removal of noise, was proposed in (Schardt et al. 2002) and in (Persson et al. 2002). The main problem of this type of approach is the determination of an optimal low pass filter for every single tree in the image. This is a kind of a chicken-and-egg problem, because the optimal low pass filter depends mainly on the diameter of the individual tree one is looking for, which is not known in advance. In (Andersen et al. 2002) the fine structure of the crown is modelled as a stochastic process with the aim to detect the underlying coarse structure of the crown.

The idea of our approach is to create a multi-scale representation of the surface model similar to (Persson et al.

2002). The difference to the approach of Persson et al. is that in our approach the scale level is *not* assumed to be known. We try to overcome the mentioned chicken-and-egg problem with a search of the “best” tree hypothesis in multiple scales. In (Brandtberg & Walter 1998) it was originally proposed to use a representation of the image data in Linear Scale Space for the extraction of individual trees. A basic idea of the Linear Scale Space is to construct a multi scale representation of an image, which only depends on one parameter and has the property of *causality*: Features in a coarse scale must have a cause in fine scale (Koenderink 1984). The scale space transformation itself may not lead to new features. One can show that a multi-scale representation based on a Gaussian function as low pass filter fulfils this requirement. In practice, the original signal $f(\vec{x})$ is convolved with a Gaussian kernel with different scale parameter σ , the result of the convolution operation is assigned as $f(\vec{x}, \sigma)$. Small values of σ correspond to a fine scale, large values to a coarse scale. An extensive investigation and mathematical reasoning including technical instructions can be found in (Lindeberg 1994).

3. DESCRIPTION OF THE APPROACH

A critical point for a successful extraction of trees is the selection of the scale level. The reasons are: (1) The correct scale level depends mainly on the size of the objects one is looking for. In the case of trees this size can neither be assumed to be known a priori nor it is constant for all trees in one image. The size of trees depends on the age, the habitat, the species and much more parameters, which cannot be modelled in advance. (2) The correct scale is of crucial importance for the segmentation. The small structures of the crown are very difficult to model and – except this small structures - the crown has a relatively elementary shape. In our approach the image is segmented in a wide range of scales, just bounded by reasonable values for the minimum and maximum diameter of a tree’s crown. In (Gong et al. 2002) the typical range for the diameter is proposed to be minimal 2.5 m up to 15 m covering all species of trees. In our experiments we increase the scale parameter in steps of about 1 m starting from 1 m up to 20 m.

As input data we use a surface model and a true orthoimage. The ground sampling distance (GSD) of the surface model is 0.25 m, it was produced by the French company ISTAR using 1:5000 colour infrared aerial images acquired in summer 2000 with a GSD of about 0.10 m, refer to (Straub & Heipke 2001) for details. A subset of the surface model is depicted in Figure 3.

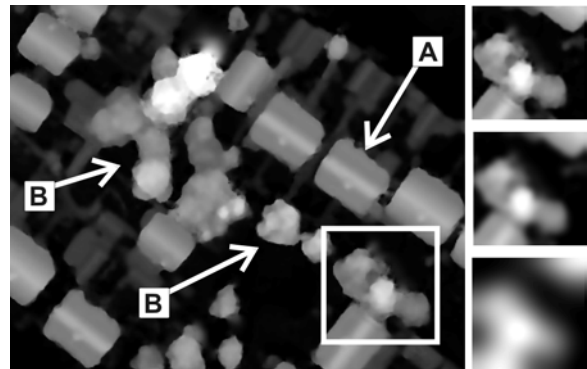


Figure 3: Surface model, buildings are marked with A and trees with B. Three different scale levels of the marked subset are depicted at the right margin.

In the following section 3.1 a detailed description of the model of individual trees is given. In section 3.2 the processing strategy for the extraction of these trees from the image and height data is described.

3.1 Model for Trees

3.1.1 Geometric Properties

The geometric part of the model for an individual tree simplifies the crown to a 2.5D surface, the Pollock-Model (Equation 1). The parameter n can be used to define the shape of a broad-leaved tree with a typical range of values from 1.0 to 1.8, and also for conifers with a typical range for n from 1.5 to 2.5. These numerical values are based on an investigation described in (Gong et al. 2002). Based on the Pollock-Model we can derive the following features for the extraction from the surface model: The projection of the model into the xy -plane is a circle with a diameter in given range. Furthermore the 3D shape of the surface is always convex.

The image processing is based on differential geometric properties. We use a profile along four tree tops to study these properties of the surface model if the trees stand close together, the normal case. Free-standing trees constitute exceptions. In the left part of Figure 4 four Pollock-Trees computed with $a=6$ [m], $b=2$ [m], and $n=2.0$ (1 m is equivalent to 10 pixels respectively grey values) are depicted.

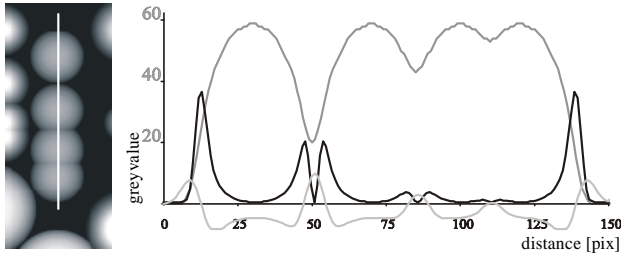


Figure 4: Profile of the surface model of four Pollock-Trees, the location of the profile is depicted in the upper left corner.

The profile is plotted in dark grey in Figure 4: One can see that the “valley” between the trees decreases from the left to the right. The absolute value of the gradient $|\nabla H(\bar{x})|$ (black line in Figure 4) decreases also. Obviously this is a consequence of the decreasing distance between the trees, and of the crown’s shape.

The surface at the tree tops has a convex shape in both directions, along and across the profile. Therefore the sum of the second partial derivations is always negative for the whole crown (refer to the light grey line in Figure 4).

$$\frac{\partial^2 H(\bar{x})}{\partial x^2} < 0 \vee \frac{\partial^2 H(\bar{x})}{\partial y^2} < 0 \Rightarrow \Delta H(\bar{x}) < 0 \quad (2)$$

At a point on the profile between two trees the partial, second derivative is smaller than zero along the profile and larger than zero perpendicular to the profile. Therefore, the Laplacian of the surface model $\Delta H(\bar{x})$ at these points has got normally higher values than at points on the crown, because both partial second derivatives are smaller than zero at the tree tops (Equation 2). These characteristics lead to local maxima between the crowns in $\Delta H(\bar{x})$.

In the case of real data this model is only valid in the convenient scale level. A height profile from real data is used to explain the term “convenient” in this context. Two different Scale Space representations of the surface model $H(\bar{x})$ are depicted in Figure 5, according to the used σ of the Gaussian they are assigned as $H(\bar{x}, \sigma)$ with σ values 0.5 m and 8 m. One can see that more and more of the fine structures disappear and the coarse structure is revealed with the increase of the scale parameter σ .

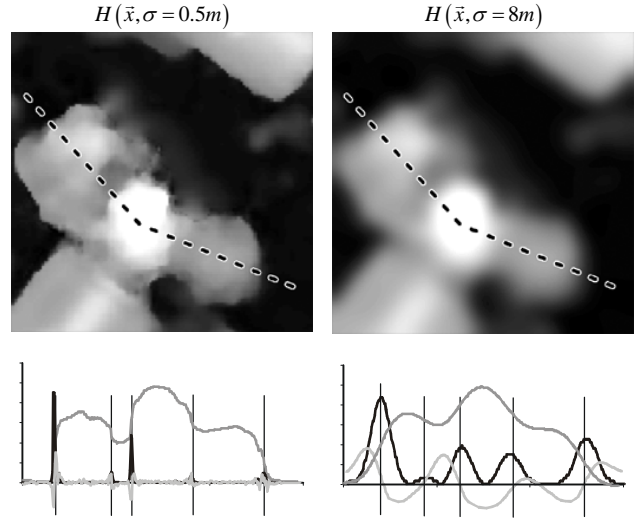


Figure 5: Representation of the surface model $H(\bar{x})$ at two different scale levels (above). The height profiles below are measured along the dotted line in the images.

The height profile along the tree tops is measured along the dotted line which is superimposed to the surface model in Figure 5. The left height profile which is measured in the original surface model is noisy compared to the profile of the synthetic trees. As a result of this noise the Laplacian is oscillating close to zero. In the “correct” scale level for this small group of trees the assumptions regarding the Laplacian are fulfilled quite well. Similar to the profile of the synthetic Pollock-Trees (Figure 4) the Laplacian is negative for trees and positive for the valleys between them. The coarse structure of the crown is enhanced, and as a result the properties of the Pollock-Model are valid also for the real trees in this scale level.

3.1.2 Reflectance Properties

Vegetation has a typical spectrum of reflection in the green and the near infrared band of the electromagnetic spectrum of wavelengths. The reflection of the near infrared band of the solar radiation is higher for vegetation than for areas without vegetation and lower in the red band. Vegetation indices make use of this typical property. If possible, we use the *Normalized Difference Vegetation Index* (NDVI) for the differentiation of vegetation and areas without vegetation in the images (refer to Figure 6 for an example).

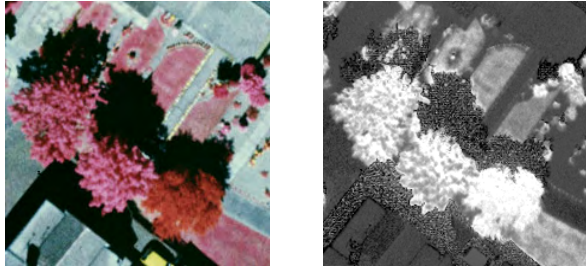


Figure 6: Colour infrared image of trees (left) and NDVI of the same area, corresponding the white square in Figure 3.

The *Degree of Artificiality*, which is computed from the green and the red band (Niederöst 2000), is an alternative if the near infrared band is not available. A purely texture based differentiation of trees and buildings can also be performed if only panchromatic images are accessible, refer to (Straub 2002).

3.2 Processing Strategy

The basis of our approach is the Linear Scale Space Theory, the Watershed transformation is used as segmentation technique, Fuzzy Sets for the evaluation of the segments and Snakes for the refinement of the crowns outline. The basic ideas of the Linear Scale Space Theory were originally proposed in (Koenderink 1984), and were worked out in (Lindeberg 1994). The Watershed transformation for the segmentation of images was introduced by (Beucher 1982). Details about the watershed transformation can be found in (Soille 1999). Fuzzy Sets (Zadeh 1965) are used, because they are a “*very natural and intuitively plausible way to formulate and solve various problems in pattern recognition.*” (Bezdek 1992). Snakes, or Active Contour Models, were introduced in (Kass et al. 1988), they “*look on nearby edges, localizing them accurately.*”

In this section we describe how to combine these tools with the aim to detect individual trees and reconstruct the outline of the crown. As mentioned above a Multi Scale Representation of the image in the Linear Scale Space is used as a basis for the approach. The main steps of the processing strategy are depicted in Figure 6:

- (1) **Segmentation:** Every scale level $H(\bar{x}, \sigma)$ of the surface model $H(\bar{x})$ is subdivided in segments B_σ using a *Watershed* transformation. The resulting segments are the *Basins* of the Watershed transformation, where σ indicates the scale level.
- (2) **Computation of membership values:** Membership values were assigned to every segment B_σ , which are partly derived from the segments itself (size and circularity), or the area

belonging to the appropriate scale level $H(\bar{x}, \sigma)$ of the surface model (curvature), and the image $I(\bar{x}, \sigma)$ (\Leftrightarrow vegetation index or texture). This results in hypothesis for trees $B_\sigma(\bar{a})$ with a feature vector \bar{a} of four fuzzy membership values.

(3) **Selection of valid hypothesis:** Every tree hypothesis $B_\sigma(\bar{a})$ is first evaluated based on the feature vector. In some cases this is leading to valid hypothesis from different scale levels which are covering each other in the xy-plane. These covering segments have to be detected and the best one according its membership value, is selected as $Tree_\sigma(\bar{a})$.

(4) The outline of the crown of every $Tree_\sigma(\bar{a})$ is measured using **Active Contours**.

3.2.1 Segmentation of the Surface Model

The segmentation of the surface model is that part of the approach which depends heavily on the scale. As mentioned above we perform a segmentation of the surface model in many scales. The segmentation procedure itself should be free of parameters and work only in the image space not in the feature space, because the feature space is independent from the scale level. The watershed transformation fulfils these requirements, and in addition it is well suited for the segmentation of height data. One reason is that the key idea of the watershed transformation is the segmentation by means of a flooding simulation (Soille 1999). *Basins* are the domains of the image which are filled up first if a water level increases from the lowest grey value in the image. *Watersheds* are embankments between the Basins. This segmentation technique is also used in (Schardt et al. 2002) and a quite similar technique in (Persson et al. 2002) with the aim of detecting individual trees.

If the watershed procedure shall be applied to extract trees from height data the surface model has to be transformed in such a way that the trees itself are basins. The easiest way to do this is to invert the surface model, as proposed in (Schardt et al. 2002). In forest areas there are usually narrow valleys between the individual crowns. In other areas, if trees occur in small groups or in rows like in settlement areas, the situation changes. Because these valleys can be very wide, the outlines of the basins are usually quite poor approximations of the crowns. Then it leads to much better results to use the edges of the surface model as segmentation function.

The watersheds of the inverted surface model are superimposed to the surface model in the left part of Figure 8, and the watersheds of the squared Laplacian of the surface model in the right part. Note, that the basins in the left Figure fit much better to the individual crowns than the basins in the right one. One can also see that if the trees stand close together – such as in

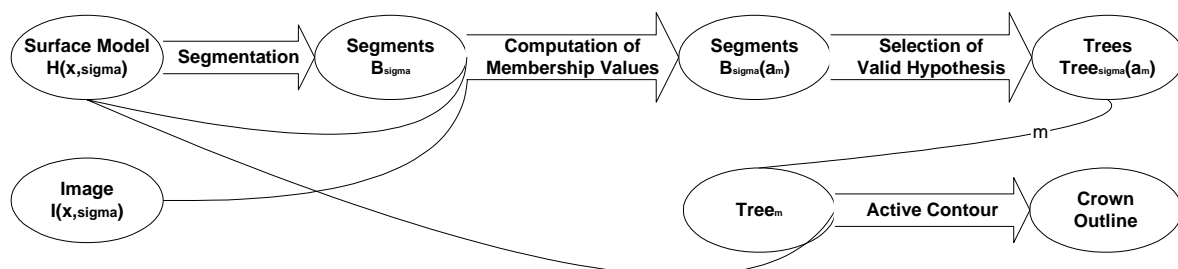


Figure 7: Processing Strategy for the extraction of trees

forest areas- the watersheds are correct. One can follow that in general the edges should be used, because this works in both cases.

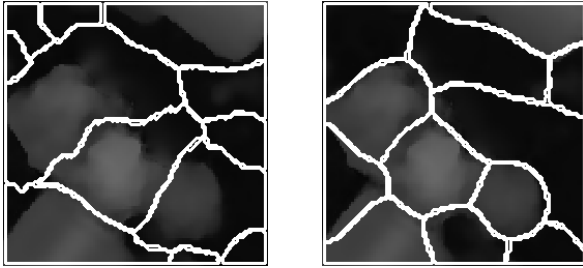


Figure 8: A subset of the surface model showing three trees (left) with superimposed watersheds of the inverted DSM (middle), the right image shows the watersheds if the edges of the surface model are used as segmentation function.

3.2.2 Computation of Membership Values

In this section we explain the four membership functions, which are used to transform the values for circularity, convexity, size and vitality (ref. Section 3.1) into membership values.

The following break points are used to define the membership function (Figure 9 left) for the **size** of a tree: The lower border is 20 m² according to a diameter of 2.5 m and the upper border is 700 m² (\Leftrightarrow 15 m). For larger values the membership value decreases, the largest possible diameter is assumed to be 35 m (\Leftrightarrow 3850 m²). The values for diameters cover all tree species, they can be found in (Gong et al. 2002). In the mentioned investigation the typical diameters are given as well as the minimum und the maximum values, which are used to define the breakpoints of the size membership function.

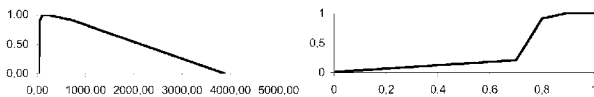


Figure 9: Size (left) and circularity (right) membership function

The **circularity** of a segment is the second feature (Figure 9 right). This feature is computed with the following formula:

$$circularity = Area(B_\sigma) / r_{max} \pi \quad (3)$$

A sensible lower border is close to the value of 0.7, the circularity value of a square. The upper border is equal 1 according to the circularity of a circle. The other breakpoint was set empirically.

The sign of the Laplacian of the surface model is used to discriminate between **convex** surfaces as trees and non-convex surfaces. For example the surfaces of building's roofs and the most ground surfaces are plane, whereas the crown of a tree is a convex surface (refer to Section 3.1.1). Thus, a negative mean value of the Laplacian within the covered area of a segment leads to a membership value of 1, and in the case of a positive mean value the membership value is 0 (Figure 10 left).

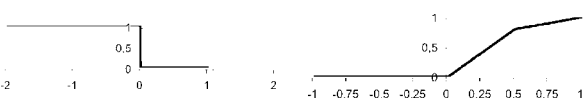


Figure 10: Convexity (left) and vitality (right) membership function

The last feature **vitality** is derived from the optical image, it is used to discriminate between vegetation and non-vegetation areas (Section 0). In this example we use the NDVI value as indicator for the vitality (Figure 10 right). Normally trees have relatively high NDVI values. Therefore we use a membership function with increasing membership value for positive NDVI values with a break point at (0.5, 0.8). The reason for this breakpoint ist that trees compared to lawn have usually a relative high NDVI value. A NDVI value of above 0.5 is a good hint for a tree.

3.2.3 Selection of Valid Hypothesis

The classification of the segments is subdivided into two steps. First, valid segments are selected according to their membership values. A tree is an object with a defined size, circularity, convexity and vitality. Consequently the minimum value of the feature vector is the value which defines if a hypothesis $B_\sigma(\vec{a})$ is a $Tree_\sigma(\vec{a})$ or not. In some cases the valid hypothesis from different scale levels can occur at a more or less identical position in the scene: Refer to Figure 11, the left image shows the valid hypothesis for trees at a scale level of $\sigma=1.9$ m and the right one at $\sigma=3.7$ m. One can see that many valid hypotheses occur in more than one scale. In some cases the segments are quite similar in both depicted scale levels, but in some other cases the segments are subdivided in the finer scale level. The trivial case – a segment in just one scale – is more an exception.

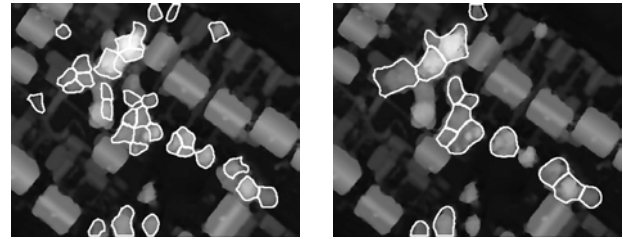


Figure 11: Valid tree segments in two different scale levels. Left: $\sigma=1.9$ m. Right: $\sigma=3.7$ m.

In the second step these different situations for every segment are analysed. Hence, the topological relation between the segments over different scale levels has to be classified. If the type of the topological relation is known, the best hypothesis for a tree can be selected at one and the same spatial position.

The classification of the topological relations between the valid segments is performed as proposed in (Winter 2000). In general, eight different topological relations exist in 2D space: *disjoint*, *touch*, *overlap*, *covers*, *contains*, *contained by*, *covers*, and *covered by* (Egenhofer & Herring 1991). These topological relations can be subdivided into two clusters $C1$ and $C2$, where the $C1$ cluster includes the relations *disjoint*, *touch* and $C2$ the other ones. The overlap relation is between these two clusters, it can be divided into *weak-overlap* ($C1$) and *strong-overlap* ($C2$) (Winter 2000). The motive behind this partitioning is that the relations in $C1$ are similar to *disjoint*, and in $C2$ to *equal*.

Here we postulate that all the segments $B_A(\vec{a})$ which have a topological relation from $C2$ to another segment $B_B(\vec{a})$, $A \neq B$ from another scale level are potential hypothesis for the **same** tree in the real world. The best hypothesis - the one with the highest membership value - is selected as $Tree_\sigma(\vec{a})$ instance. Accordingly, both investigated hypothesis are

assumed as valid if the relation between the two segments is from CI .

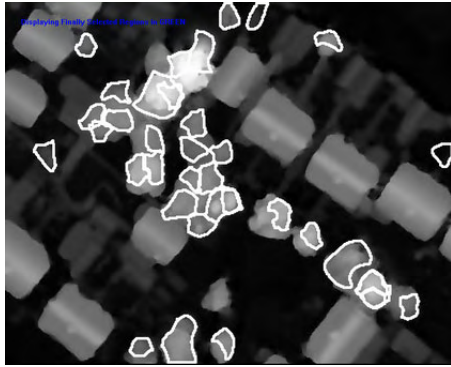


Figure 12: Selected segments superimposed to the surface model, the white lines depict the best segments over all investigated scales.

The selected hypotheses are depicted in Figure 12. The white lines correspond to the outlines of the segments, which are selected as valid trees (compare Figure 11). Most of the trees in the scene were detected correctly, but many of the boundaries are not really good approximations for the outline of the individual crowns. The reason for the worse approximation of the outline is that the feature circularity is relatively weak for small segments on the one hand, and on the other hand it is the main decision instance between segments at the same location, if the size, the vitality, and the convexity criterion have similar or equal membership values. This occurs often, if the crown consists of more than one sub-crown. This leads over to the last processing step: The outlines of the crowns will be refined with Active Contours.

3.2.4 Measurement of the Outline

The outlines of the segments were extracted in different scale levels. But the outline of the crown is an object without a changing scale, as distinct from the crown itself. In order to take this into account, the outline of the crown is measured in the fine scale with the help of an *Active Contour Model*, respectively a *Snake*. A Snake is a deformable geometric model with physical properties like elasticity. It is a kind of a virtual rubber cord which can be used to detect valleys in a hilly landscape with the help of gravity. If the Snake is initialised close to the valleys of the landscape, the gravity causes a movement to the valleys. The “landscape” may be a surface model, an image, or the edges of an image. The movement originates in a field of gradients, which can be computed on the base of an edge detectors result. Compare Figure 13: In the background one can see the edges of a circular object, the enlargement in the foreground shows the field of gradient vectors. The source of the gradient field is usually assigned as external force or external energy.

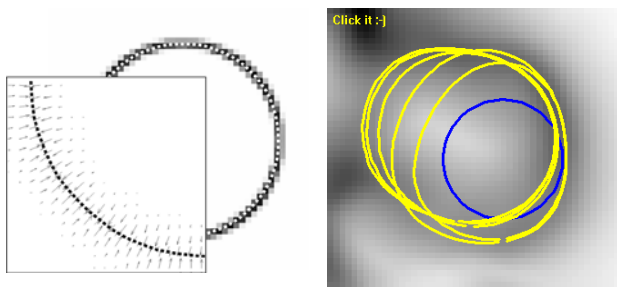


Figure 13: Left: External force for a Snake (background) and the resulting field of gradients which controls the movement of a Snake (foreground). Right: Example for the measurement of the outline with a Snake. Five different optimisation steps are depicted.

Snakes were originally introduced by (Kass et al. 1988) as mid-level algorithm which combines geometric and/or topologic constraints with the extraction of low-level features from images. The principal idea is to define a contour with the help of mechanic properties like elasticity and rigidity, to initialise this contour close to the boundary of the object one is looking for, and then let the contour move into the direction of the boundary of the objects. The original energy based approach for the contour can be reformulated to a pure geometry based approach, called Geodesic Active Contours (Caselles et al. 1997). Recent developments combine Geodesic Active Contours with level set methods (Paragios & Deriche 2002), then the topology of the Active Contour can change during the optimisation.

In general, there are two main drawbacks for the application of Snakes as measurement tool. The first one is that the Snake has to be initialised very close to the features one is looking for. Otherwise the behaviour of the Snake is nearly impossible to predict. The second one is the tuning of the parameters, primarily the weighting between internal and external forces and the selection of the external force field itself.

In our approach the Snake is used only for the fine measurement in the last stage, the coarse shape of the crown is more or less known. Furthermore we know that the approximation is often too small. Based on these constraints we could build a Snake which is quite stable under this special conditions: The geometry of the Snake is initialised for every $Tree_{\sigma}(\bar{a})$ as circular shaped closed polygon at the gravity centre of the appropriate Basin B_{σ} . This initialisation stage is depicted in Figure 12 as grey (blue) circle in the left image. The parameters for the internal energies were tuned such that the length of the contour is low, and the curvature a high weighted. Without external forces, a Snake which is tuned in such a way converges to a circle with a trend to decrease its length². As the approximation is often too small (see last section) an additional force is added, which makes the Snake behave like a balloon (Cohen 1991). With this additional force the contour moves towards the outline of the crown even if no external forces influence the movement. As external force we use the absolute value of the gradients $|\nabla H(\bar{x}, \sigma)|$. In order to enhance the capture range of the gradients in the fine scale (refer to Figure 14 left) we use the sum of the gradients absolute values over all scale levels. The fine scale edges are preserved and the capture range is enhanced, compared to the fine scale edges alone (refer to Figure 14 right).

At least, the membership values of every $Tree_{\sigma}(\bar{a})$ has to be computed again because its outlines have changed. Even the topological relations between the tree hypotheses are no longer valid and have to be computed again. Furthermore, a changing

² The weighting parameter *alpha* for the first order term of the internal energy is set to low values close to zero, the parameter *beta* for the second order term has a high weight. According to the classical notion of (Kass et al. 1988).

of the topology occurs if the segments $B_\sigma(\bar{a})$ correspond to two or more parts of the same crown in the real world.

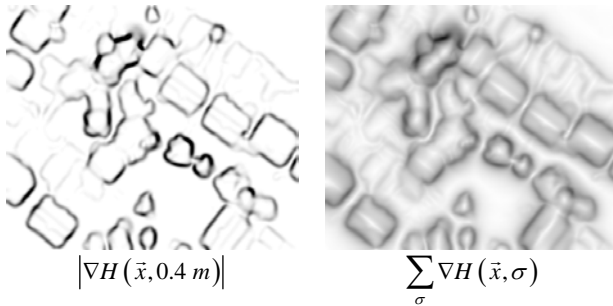


Figure 14: Examples for different external forces fields.

In these cases, the Snake converges usually to an identical solution for every of these parts. And this again leads to the change of the topological relation from the C1 cluster (similar to *disjoint*) to the C2 cluster (similar to *equal*). The updated membership values are quite independent from the pre-processing in the different scale levels. Therefore these values are well suited as internal evaluation of the tree hypotheses.

4. RESULTS

The results of the whole approach are depicted in Figure 14, every $Tree_\sigma(\bar{a})$ as one circle. The position of the $Tree_\sigma(\bar{a})$ is the centre of gravity of its outline, and the radius is computed based on the outline's length. The valid instances are plotted in black, the white circles are the hypothesis which are looked upon as not valid. The instances, which are marked with an "A" in Figure 15, are examples for the situation as mentioned above: A crown which was split into two or more segments was correctly delineated by the Snake, and as a result the redundant instances were removed. In the "B"-marked situation a true positive was removed, because it was *strong overlapped* by another instance. The "C"-marked instances are evaluated as not valid because the membership value after the re-computation is too low.

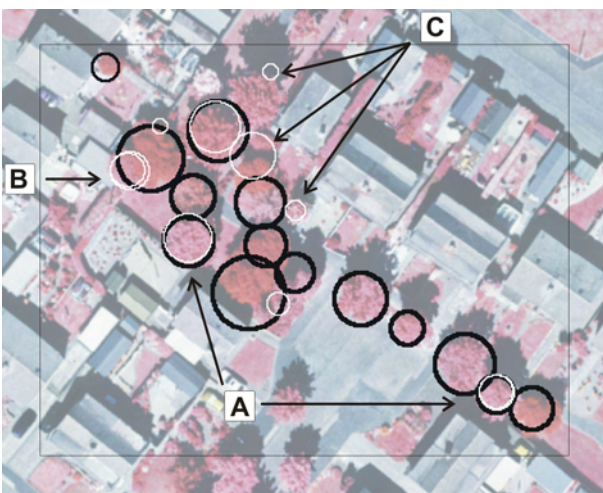


Figure 15: Final results of the approach. Valid hypothesis for trees are depicted as black circles, non-valid hypothesis as white circles.

The results as depicted in Figure 15 are typical for the approach if the membership functions were not tuned for a special scene. The values for the size stem from an independent investigation

(Gong et al. 2002), and the convexity is always positive. Only the breakpoints in the circularity membership function are more or less heuristic values. The breakpoint for the vitality has to be selected manually. Under this pre-conditions the results are convincing.

5. SUMMARY AND OUTLOOK

An approach for the automatic extraction of trees from a true orthoimage and a digital surface model was presented in this paper. The approach is free of a priori assumptions about the scale level in which the trees are represented ideally. The relevance of the scale level has been worked out in the paper. The segmentation is performed in a wide range of scale levels, and the evaluation of the segments is independent from the scale. The approach is free of assumptions about the terrain, because the height of the trees is not used for the detection. This is important to note, as it is a difficult task to extract the ground surface in forest areas automatically. And finally the classification of the hypothesis is based on not more than four parameters: size, circularity, convexity, and vitality. From these four parameters only one depends of the used image material, the other ones are object properties. The measurement of the crown's outline is performed with a Snake. The tuning of the parameters for the Snake algorithm is a difficult task, but once adjusted it works stable as measurement tool without changing these settings if the input data and/or the context changes. The approach was tested on different larger data sets, which can be found in (Straub 2003a) (Straub 2003b).

Further developments should focus on the evaluation of the tree hypothesis. The highest potential is expected by a refinement of the membership functions with the help of statistical investigations on large data sets. The detection of the individual trees and the measurement of the outline can be looked upon as a bottleneck for the further classification of trees. Based on these, further information about the 3D shape of the crown or the fine structure characteristics of the individual tree can be extracted in the future.

ACKNOWLEDGEMENT

Parts of this work were founded by the European Commission under the contract IST-1999-10510.

REFERENCES

- Andersen, H., Reutebusch, S. E., Schreuder, G. F., 2002. Bayesian Object Recognition for the Analysis of Complex Forest Scenes in Airborne Laser Scanner Data. *International Archives of the Photogrammetry, Remote Sensing and Spatial Information Sciences*, (eds.) Kalliany Leberl, ISPRS, Graz, Austria, Vol. XXXIV, Nr. WG 3A, pp. 35-41.
- Beucher, S., 1982. Watersheds of Functions and Picture Segmentation. *International Conference on Acoustics, Speech and Signal Processing*, IEEE, Paris, pp. 1928-1931.
- Bezdek, J. C., 1992. Computing with Uncertainty. *IEEE Communications Magazine*, September (1992), pp. 24-36.
- Brandtberg, T., 1999. Structure-based classification of tree species in high spatial resolution aerial images using a fuzzy clustering technique. *The 11th Scandinavian Conference on Image Analysis*, Kangerlussueq, Greenland, June 7-11, pp. 165-172.

- Brandtberg, T., Walter, F., 1998. Automated delineation of individual tree crowns in high spatial resolution aerial images by multiple scale analysis. *Machine Vision and Applications*, 11 (1998), pp. 64-73.
- Caselles, V., Kimmel, R., Sapiro, G., 1997. Geodesic Active Contours. *International Journal of Computer Vision*, 1 (22), pp. 61-79.
- Cohen, L., 1991. On active contour models and balloons. *CVGIP: Image Understanding*, 2 (53), pp. 211-218.
- Egenhofer, M. J., Herring, J. R., 1991. Categorizing Binary Topological Relations Between Regions, Lines, and Points in Geographic Databases. University of Maine, National Center for Geographic Information and Analysis, Orono, Maine, USA, pp. 28.
- Gong, P., Sheng, Y., Biging, G., 2002. 3D Model Based Tree Measurement from High-Resolution Aerial Imagery. *Photogrammetric Engineering & Remote Sensing*, 11 (68), pp. 1203-1212.
- Gougeon, F., Moore, T., 1988. Individual Tree Classification Using Meis-II Imagery. *IGARSS '88 Geoscience and Remote Sensing Symposium*, IEEE, Vol. 2, pp. 927 -927.
- Hildebrandt, G., 1987. 100 Jahre forstliche Luftbildaufnahme - Zwei Dokumente aus den Anfängen der forstlichen Luftbildinterpretation. *Bildmessung und Luftbildwesen*, 55 (1987), pp. 221-224.
- Hyypä, J., Hyypä, H., Ruppert, G., 2000. Automatic Derivation of Features to Forest Stand Attributes Using Laser Scanner Data. *International Archives of Photogrammetry and Remote Sensing*, ISPRS, Amsterdam, Vol. XXXIII, Nr. Part B3, pp. 421-428.
- Kass, M., Witkin, A., Terzopoulos, D., 1988. Snakes: Active Contour Models. *International Journal of Computer Vision*, 1 (1988), pp. 321-331.
- Koenderink, J., 1984. The Structure of Images. *Biological Cybernetics*, (50), pp. 363-370.
- Larsen, M., 1999. Individual tree top position estimation by template voting. *21. Canadian Symposium on Remote Sensing*, Ottawa, Canada, 21-24 June, pp. 8.
- Lillesand, T. M., Kiefer, R. W., 1994. *Remote Sensing and Image Interpretation*. John Wiley & Sons, New York Chichester Brisbane Toronto Singapore, pp. 750.
- Lindeberg, T., 1994. *Scale-Space Theory in Computer Vision*. Kluwer Academic Publishers, Boston, USA, pp. 423.
- Niederöst, M., 2000. Reliable Reconstruction of Buildings for Digital Map Revision. *International Archives Photogrammetry and Remote Sensing*, ISPRS, Amsterdam, Netherlands, Vol. XXXIII, Nr. Part B3, pp. 635-642.
- Paragios, N., Deriche, R., 2002. Geodesic Active Regions and Level Set Methods for Supervised Texture Segmentation. *International Journal of Computer Vision*, 3 (46), pp. 223-247.
- Persson, A., Holmgren, J., Söderman, U., 2002. Detecting and Measuring Individual Trees Using an Airborne Laser Scanner. *Photogrammetric Engineering & Remote Sensing*, 9 (68), pp. 925-932.
- Pinz, A., 1989. Final Results of the Vision Expert System VES: Finding Trees in Aerial Photographs. *Proceedings ÖAGM 13. Workshop of the Austrian Association for Pattern Recognition*, Oldenbourg Schriftenreihe Österreichische Computer Gesellschaft, Wien München, pp. 90-111.
- Pollock, R. J., 1994. A model-based approach to automatically locating tree crowns in high spatial resolution images. *Image and Signal Processing for Remote Sensing*, (eds.) Desachy, SPIE, Vol. 2315, pp. 526-537.
- Pollock, R. J., 1996. The Automatic recognition of Individual trees in Aerial Images of Forests Based on a Synthetic Tree Crown Image Model. *Dissertation Computer Science*, The University of British Columbia, Vancouver, Canada, June 1996, pp. 170.
- Saint John, R. W., 1997. Building the Perfect Tree A Lesson in Optimization an PROTO. <http://www.vrmlsite.com/jun97/a.cgi/spot2.html>, 3-20-2003,
- Schardt, M., Ziegler, M., Wimmer, A., Wack, R., Hyypä, R., 2002. Assessment of Forest Parameter by Means of Laser Scanning. *International Archives of the Photogrammetry, Remote Sensing and Spatial Information Sciences*, (eds.) Kalliany Leberl, ISPRS, Graz, Austria, Vol. XXXIV, Nr. 3A, pp. 302-309.
- Schneider, S., 1974. *Luftbild und Luftbildinterpretation*. de Gruyter, Berlin New York, pp. 530.
- Soille, P., 1999. *Morphological Image Analysis: Principles and Applications*. Springer, Berlin Heidelberg New York, pp. 316.
- Straub, B., 2002. Investigation of the MPEG-7 Homogeneous Texture Descriptor for the Automatic Extraction of Trees. *International Archives of the Photogrammetry, Remote Sensing, and Spatial Information Sciences*, (eds.) Kalliany, ISPRS, Graz, Austria, September 9-13, Vol. XXXIV, Nr. 3A, pp. 351-355.
- Straub, B., 2003. A Top-Down Operator for the Automatic Extraction of Trees - Concept and Performance Evaluation. *The International Archives of the Photogrammetry, Remote Sensing and Spatial Information Sciences*, (eds.) Hans-Gerd Maas George Vosselmann, ISPRS, Dresden, Germany, pp. (accepted). (b)
- Straub, B., 2003. Automatic Extraction of Trees from Height Data using Scale Space and Snakes. *Second International Precision Forestry Symposium*, Precision Forestry Cooperative, Seattle, USA, 15.-18. Juni, pp. (in print). (a)
- Straub, B., Heipke, C., 2001. Automatic Extraction of Trees for 3D-City Models from Images and Height Data. *Automatic Extraction of Man-Made Objects from Aerial and Space Images*. Vol. 3. ed. Baltasavias Gruen van Gool, A.A.Balkema Publishers. Lisse Abingdon Exton(PA) Tokio. pp. 267-277.
- Winter, S., 2000. Uncertain Topological Relations between Imprecise Regions. *International Journal of Geographic Information Science*, 5 (14), pp. 411-430.
- Zadeh, L., 1965. Fuzzy Sets. *Information and Control*, 3 (8), pp. 338-353.